Utilizing Machine Learning for Identifying Quantum-Many-Body Phase Transitions

Ron Ziv*[a], **David Wei**[b], **Antonio Rubio-Abadal**[b], **Anna Keselman**[a], **Eran Lustig**[c], **Johannes Zeiher**[b], **Ronen Talmon**[a], **Immanuel Bloch**[b], **Mordechai Segev**[a]

[a] *Technion - Israel Institute of Technology,3200003 Haifa, Israel* ronziv@campus.technion.ac.il

[b] *Max-Planck-Institut für Quantenoptik & Ludwig-Maximilians-Universität München, 80799 Munich, Germany*

[c] *Edward L. Ginzton Laboratory, Stanford University, Stanford, 94305, CA, USA.*

*Presenting author

1. Introduction

Phase transitions represent fundamental changes in the behavior of physical systems under small modifications to external parameters. Examples range from metal–insulator [1], gas–liquid [2], and topological transitions [3] to transitions in quantum many-body (QMB) systems[4]. Deciphering the conditions of such transitions, i.e., finding the specific regimes under which a transition occurs, is important both to basic science and to technology, as different phases introduce different characteristics that can be exploited as a resource.

Generally, phase transitions occur not only in the classical regime, driven by classical (or semiclassical) interactions between the physical constituents of the system, but also in QMB systems, where the task of identifying the phase transition is especially hard and challenging due to the exponential growth of the Hilbert space with the number of particles. Namely, in a many-body system of 100 quantum particles, even if each particle is a two-level system, the number of observables is 2^{2N}, which renders their measurement impractical. Moreover, identifying QMB phase transitions from experimental data is also extremely hard: the available measurements tend to always be incomplete, and indicators of a phase transition are not always clear [5, 6].

Over the years, various theoretical measures for detecting phase transitions have been proposed [7, 8, 9]. However, experimental constraints often limit the number of accessible observables, making the direct application of these theoretical metrics challenging. For instance, in many quantum gas microscope experiments used to study QMB systems, the primary measurable quantity is atoms per site [10, 11]. This restriction hinders the full characterization of the high-dimensional density matrix and, consequently, the computation of these theoretical measures. Due to these measurement limitations, alternative approaches are often employed. For example, in many-body localization (MBL) experiments, the persistence of an initially engineered state's imbalance serves as a heuristic for detecting behavioral changes. However, this method depends on specific initial state choices (e.g., a sharp edge in the density of atoms) [12, 13] and lacks universality. Thus, there is a clear need for a robust, measurement-agnostic framework capable of detecting phase transitions directly from raw experimental data.

Here, we present a novel, unsupervised data-driven approach that leverages manifold learning, Our method is derived from the Diffusion Maps (DM) algorithm [14], adjusted specifically to detect phase transitions from raw experimental snapshots without any prior knowledge of labels or physical observable (e.g., entanglement or density matrices). ***The key aspect of our methodology lies in tailoring DM to quantum data:***

- **Repeated Quantum Measurements:** Operating on ensemble of raw snapshots from each experimental setting, handling the probabilistic nature of quantum measurements.
- **State-Agnostic and Measurement-Agnostic Framework.** Our method does not hinge on a specific initial state configuration or a certain subset of observables. This is especially useful in cases where the experiment only provides partial information, such as site parity.
- **Experimental validation**: We validate our algorithm on experimental data from quantum simulators of Bose-Hubbard models and quantum gas microscope experiments, detecting phase transitions in real experimental settings.

2. Background and related work

Recent years have witnessed a surge in machine learning (ML) methods for phase transition detection in both classical and quantum systems [15, 16, 17, 18, 19]. In practice, supervised ML approaches are of limited use for experimental data lacking clear labels (i.e., known phase identities), and such labels simply do not exist for QMB system. Moreover, even hybrid solutions— where simulated data labels are used to guide experimental classification—generally fail because simulations diverge for large quantum systems (which is exactly the reason why quantum simulators have been proposed). Consequently, the most promising approaches rely on unsupervised ML [20, 21, 22], that can be applied to experimental measurements directly.

Another prominent avenue relies on traditional machine learning techniques such as manifold learning and kernel methods. These approaches assume that high-dimensional data lie on a lower dimensional manifold that can be uncovered by analyzing intrinsic geometry. Although these methods can be less expressive compared to deep neural networks, they often require fewer training samples and are more straightforward to utilize, making them attractive for a wide range of experimental scenarios[23, 24].

3. Methods and Results

Diffusion Maps for Quantum Experiments Our technique for identifying phase transitions in quantum many-body systems is inspired by the DM algorithm [14]. In DM, one constructs a kernel (similarity matrix) based on pairwise distances between data points. By normalizing this kernel to be row-stochastic and then performing an eigendecomposition, one obtains a new embedding of the data in a low dimensional space spanned by the leading eigenvectors. Distances in this diffusion space reflect the intrinsic geometry of the original data. However, unlike in the classical settings, quantum experiments introduce additional complexity as each parameter setting S_i (e.g., a particular value of interaction strength) is represented by multiple measurement snapshots due to the probabilistic nature of quantum measurements. Formally, we have $\mathcal{S} = \{S_1, S_2, \ldots, S_n\}$, $S_i = \{p_1^{(i)}, p_2^{(i)}, \ldots, p_m^{(i)}\}$, where each snapshot $p_j^{(i)} \in \mathcal{X}$ lies in some measurement space (*e.g.*, single-site occupations).

Kernel Construction Directly averaging snapshots in the original measurement space fails to capture the true geometry. Inspired by our previous work [25], we instead adopt a Mahalanobis-like distance [26] between the *distributions* of snapshots: $d^2(z_i, z_j) = \frac{1}{2}(z_i - z_j)^\top \left(C_i + C_j\right)^{-1}(z_i - z_j)$ Where $z_i = \frac{1}{m}\sum_{j=1}^{m} p_j^{(i)}$ and C_i is the empirical covariance of S_i. A similarity function $f(\cdot)$ then gives the kernel $K(S_i, S_j) = f\left(d^2(z_i, z_j)\right)$ The resulting kernel is used to construct the DM embedding. This procedure embeds each multi-snapshot data set S_i into a *single point* in latent space.

Detection Metric To identify phase transitions, we embed each set S_i into the low-dimensional space and look for sharp changes or clustering in the embedding. Concretely :

- *Spectral Gap & Cluster Separation*: Large spectral gaps eigenvalues and abrupt changes in distances between clusters of points in latent space may indicate natural partitions corresponding to different phases.
- *Order Parameters in Embedding*: We empirically observe that in some cases, a single latent coordinate may serve as an emergent order parameter, like in the case of simulated Ising model (Appendix A).

Results For brevity, we present here results on two cases and elaborate in more detail in Appendix. To demonstrate the performance and utility of our approach, we first test it on a classical $2D$ Ising system with 128^2 spin sites that can be simulated on a classical computer for $100 >$ particles. Here, each initial configuration of the system is considered a snapshot to match the probabilistic quantum case, and the varying parameter is the temperature. We find excellent agreement with the simulated results placing the transition at $T_c = 2.33 \pm 0.05[\frac{J}{k_B}]$. We then apply our methodology to data from an experiment probing a $2D$ disordered Bose-Hubbard system undergoing an MBL transition [27]. The experiment consists of 250 particles, hence it cannot be simulated on a classical computer. Here is where our method comes into play: our embedding and transition-detection method identifies the presence of a phase transition, with critical disorder, W, closely matching the heuristic estimate reported in the original experiment where we see an imbalance trend change at $W \approx 5[J]$ with complete transition to MBL at $W \approx 15[J]$. For more details, Appendix B

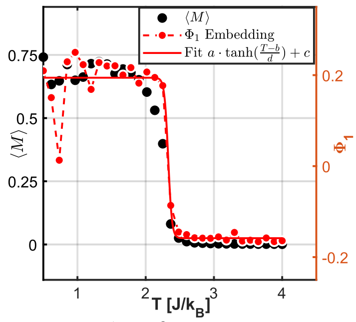

Fig. 1: Ising system, plot of magnetism versus the leading embedding coordinate.

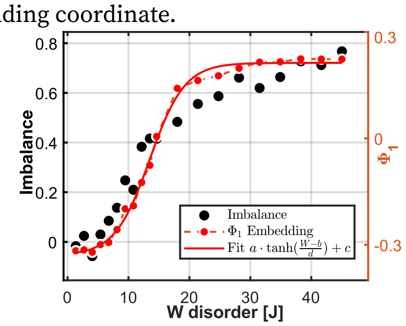

Fig. 2: Many-Body Localization, plot of imbalance heuristic versus the leading embedding coordinate.

4. Conclusion & Outlook

Our diffusion-maps-based method provides an unsupervised, measurement-agnostic, and state agnostic framework to detect quantum phase transitions directly from raw experimental data. Its computational efficiency and minimal assumptions make it ideally suited for rapid, exploratory analysis in quantum experiments, where establishing a clear phase metric is challenging. Going forward, since our methodology is universal – not restricted to a specific platform - we anticipate broader applications across different QMB platforms. Finally, we envision integrating our method with active experimental feedback loops to guide the measurements and eventually use the combined method to extract the physical features of the phase transition, beyond what we did here – identifying the presence of the phase transition and the parameters at which the transition occurs.

Acknowledgments

Ron Ziv acknowledges the support of Israel's Council of Higher Education PhD fellowship in Quantum Science and Technology.

References

[1] F. J. Morin. Oxides Which Show a Metal-to-Insulator Transition at the Neel Temperature. *Physical Review Letters*, 3(1):34–36, July 1959.

[2] M. W. Kim and D. S. Cannell. Experimental study of a two-dimensional gas-liquid phase transition. *Physical Review A*, 13(1):411–416, January 1976.

[3] B. A. Bernevig, T. L. Hughes, and S.-C. Zhang. Quantum Spin Hall Effect and Topological Phase Transition in HgTe Quantum Wells. *Science*, 314(5806):1757–1761, December 2006.

[4] M. Vojta. Quantum phase transitions. *Reports on Progress in Physics*, 66(12):2069, November 2003.

[5] R. K. Panda, A. Scardicchio, M. Schulz, S. R. Taylor, and M. Žnidarič. Can we study the many-body localisation transition? *EPL (Europhysics Letters)*, 128(6):67003, February 2020.

[6] P. Sierant and J. Zakrzewski. Challenges to observation of many-body localization. *Physical Review B*, 105(22):224203, June 2022.

[7] N. C. Murphy, R. Wortis, and W. A. Atkinson. Generalized inverse participation ratio as a possible measure of localization for interacting systems. *Physical Review B*, 83(18):184206, May 2011.

[8] M. Serbyn, Z. Papić, and D. A. Abanin. Criterion for Many-Body Localization-Delocalization Phase Transition. *Physical Review X*, 5(4):041047, December 2015.

[9] J. Eisert, M. Friesdorf, and C. Gogolin. Quantum many-body systems out of equilibrium. *Nature Physics*, 11(2):124–130, February 2015.

[10] S. Bakr, W, J. I. Gillen, A. Peng, S. Fölling, and M. Greiner. A quantum gas microscope for detecting single atoms in a Hubbard-regime optical lattice. *Nature*, 462(7269):74–77, November 2009.

[11] J. F. Sherson, C. Weitenberg, M. Endres, M. Cheneau, I. Bloch, and S. Kuhr. Single-atom-resolved fluorescence imaging of an atomic Mott insulator. *Nature*, 467(7311):68–72, September 2010.

[12] Y. Bar Lev and D. R. Reichman. Dynamics of many-body localization. *Physical Review B*, 89(22):220201, June 2014.

[13] Y. Prasad and A. Garg. Initial state dependent dynamics across the many-body localization transition. *Physical Review B*, 105(21):214202, June 2022.

[14] R. R. Coifman and S. Lafon. Diffusion maps. *Applied and Computational Harmonic Analysis*, 21(1):5–30, July 2006.

[15] J. Carrasquilla and R. G. Melko. Machine learning phases of matter. *Nature Physics*, 13(5):431–434, May 2017.

[16] A. Tanaka and A. Tomiya. Detection of Phase Transition via Convolutional Neural Networks. *Journal of the Physical Society of Japan*, 86(6):063001, June 2017.

[17] A. Bohrdt, C. S. Chiu, G. Ji, M. Xu, D. Greif, M. Greiner, E. Demler, F. Grusdt, and M. Knap. Classifying snapshots of the doped Hubbard model with machine learning. *Nature Physics*, 15(9):921–924, September 2019.

[18] E. Lustig, O. Yair, R. Talmon, and M. Segev. Identifying Topological Phase Transitions in Experiments Using Manifold Learning. *Physical Review Letters*, 125(12):127401, September 2020.

[19] H.-Y. Huang, R. Kueng, and J. Preskill. Predicting many properties of a quantum system from very few measurements. *Nature Physics*, 16(10):1050–1057, October 2020.

[20] E. P. L. van Nieuwenburg, Y.-H. Liu, and S. D. Huber. Learning phase transitions by confusion. *Nature Physics*, 13(5):435–439, May 2017.

[21] P. Huembeli, A. Dauphin, P. Wittek, and C. Gogolin. Automated discovery of characteristic features of phase transitions in many-body localization. *Physical Review B*, 99(10):104106, March 2019.

[22] K. Kottmann, P. Huembeli, M. Lewenstein, and A. Acín. Unsupervised Phase Discovery with Deep Anomaly Detection. *Physical Review Letters*, 125(17):170603, October 2020.

[23] U. Yang, Z.-Z. Sun, S.-J. Ran, and G. Su. Visualizing quantum phases and identifying quantum phase transitions by nonlinear dimensional reduction. *Physical Review B*, 103(7):075106, February 2021.

[24] Y. Che, C. Gneiting, T. Liu, and F. Nori. Topological quantum phase transitions retrieved through unsupervised machine learning. *Physical Review B*, 102(13):134213, October 2020.

[25] R. Ziv, A. Rubio-Abadal, A. Keselman, R. Talmon, I. Bloch, and M. Segev. Machine Learning Detection of Quantum Many-Body Localization Phase Transition. In *Conference on Lasers and Electro-Optics (2022)*, page FF2I.3, May 2022.

[26] R. Talmon and R. R. Coifman. Empirical intrinsic geometry for nonlinear modeling and time series filtering. *Proceedings of the National Academy of Sciences*, 110(31):12535–12540, 2013.

[27] J.-Y. Choi, S. Hild, J. Zeiher, P. Schauß, A. Rubio-Abadal, T. Yefsah, V. Khemani, D. A. Huse, I. Bloch, and C. Gross. Exploring the many-body

localization transition in two dimensions. *Science*, June 2016.

Appendix A. Ising

We simulate an $2D$ Ising model on a square lattice with nearest neighbour interactions. The system consists of $L \times L$ spins, $S_i = \pm 1$ arranged in a plane where we take $L = 128$. The Hamiltonian is given by:

$$H = -J \sum_{\langle i,j \rangle} S_i S_j$$

Where S_i is the spin at site i, and J is the nearest neighbour interaction strength. The system is initialized in a random spin configuration and evolves at a finite temperature. We utilized the Metropolis algorithm to sample the system at different temperatures. After a sufficient number of steps, we compute the magnetization for that specific configuration given by:

$$\langle M \rangle = \frac{1}{L^2} \sum_i S_i$$

To align with the probabilistic setting of the QMB systems, for each temperature we repeat the above for many initial lattice configurations. This allows us to form a set of snapshots per temperature for the algorithm. The magnetization order parameter was averaged over all snapshots to produce a final value per temperature point. Empirically, we observe good agreement between the order parameter of the system and the first latent coordinate of the algorithm. To detect the transition point we fit the latent coordinate to

$$a \cdot tanh(\frac{T-b}{d}) + c$$

where b identifies the crossing point and the other parameters are used for fit scaling and shifting. In our settings, we obtain critical temperature of $T_c = 2.33 \pm 0.05[J/k_B]$. In good agreement with known value given by $T_c \approx 2.269[J/k_B]$. Of course, the fitting criteria is a physics motivated design choice, but other criteria can be selected to cluster the different phases in the latent space.

Appendix B. Bose-Hubbard results

Our experimental system is a $2D$ lattice of cold bosonic atoms in a single plane under a harmonic trap, with radius roughly given by 9 lattice sites. A disorder pattern is projected on the system with a random potential in each site. The system starts in a unit filled Mott insulator state and undergoes a quench, the lattice depth is lowered to allow evolution and interaction between the atoms in each site. During the evolution the dynamics can be described by the $2D$ BH Hamiltonian with onsite disorder described by the following equation:

$$H = -J \sum_{\langle i,j \rangle} \hat{a}_i^\dagger \hat{a}_j + \frac{U}{2} \sum_i \hat{n}_i(\hat{n}_i - 1) + W \sum_i \delta_i \hat{n}_i.$$

where $\hat{a}_i^\dagger$ ($\hat{a}_j$) is the bosonic creation(annihilation) operator, n_i is the local density operator of site i, δ_i is random disorder potential of site i, and W is its amplitude. Here J represents the hopping strength between nearest neighbor sites, and U gives the onsite interaction strength. After the quench, the atoms are allowed to evolve freely, followed by a site resolved parity measurement. In the experimental system, the system was initialized with an artificial edge by removing half of the atoms from one side of the trap, creating an imbalanced state. The imbalance per disorder point was measured by:

$$Imbalance = \frac{N_L - N_R}{N_{total}}$$

Computing the difference between the total atoms on the right and left of the artificial edge.

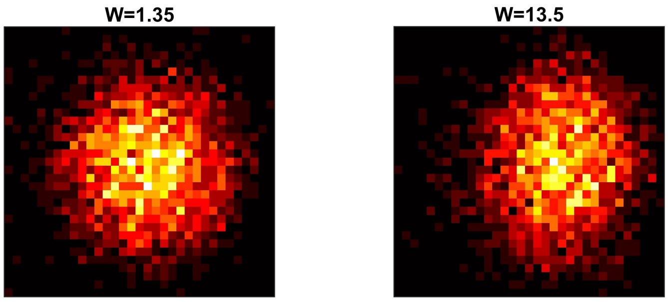

Fig. B1: Mean measurements for two different disorder strengths.

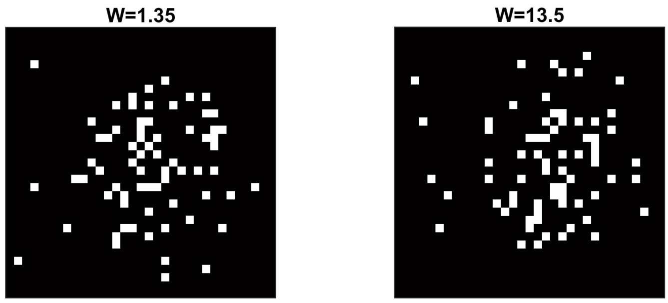

Fig. B2: Single snapshot measurements for two different disorder strengths.